NRIAG Journal of Astronomy and Geophysics 6 (2017) 131–140

Contents lists available at ScienceDirect

NRIAG Journal of Astronomy and Geophysics

journal homepage: www.elsevier.com/locate/nrjag

Full length article

Investigation of geomagnetic induced current at high latitude during the storm-time variation

E.O. Falayi [a,*], O. Ogunmodimu [b], O.S. Bolaji [c], J.D. Ayanda [a], O.S. Ojoniyi [a]

[a] Department of Physics, Tai Solarin University of Education, Ijagun, P.M.B 2118, Ijebu Ode, Ogun State, Nigeria
[b] Department of Physics, Lancaster University, Lancaster, United Kingdom
[c] Department of Physics, University of Lagos, Akoka, Nigeria

ARTICLE INFO

Article history:
Received 8 December 2016
Revised 25 April 2017
Accepted 27 April 2017
Available online 5 May 2017

Keywords:
Geomagnetically induced currents (GIC)
Time derivatives of the geomagnetic field (dB/dt)
Geomagnetic disturbances and correlation coefficients

ABSTRACT

During the geomagnetic disturbances, the geomagnetically induced current (GIC) are influenced by the geoelectric field flowing in conductive Earth. In this paper, we studied the variability of GICs, the time derivatives of the geomagnetic field (dB/dt), geomagnetic indices: Symmetric disturbance field in H (SYM-H) index, AU (eastward electrojet) and AL (westward electrojet) indices, Interplanetary parameters such as solar wind speed (v), and interplanetary magnetic field (Bz) during the geomagnetic storms on 31 March 2001, 21 October 2001, 6 November 2001, 29 October 2003, 31 October 2003 and 9 November 2004 with high solar wind speed due to a coronal mass ejection. Wavelet spectrum based approach was employed to analyze the GIC time series in a sequence of time scales of one to twenty four hours. It was observed that there are more concentration of power between the 14–24 h on 31 March 2001, 17–24 h on 21 October 2001, 1–7 h on 6 November 2001, two peaks were observed between 5–8 h and 21–24 h on 29 October 2003, 1–3 h on 31 October 2003 and 18–22 h on 9 November 2004. Bootstrap method was used to obtain regression correlations between the time derivative of the geomagnetic field (dB/dt) and the observed values of the geomagnetic induced current on 31 March 2001, 21 October 2001, 6 November 2001, 29 October 2003, 31 October 2003 and 9 November 2004 which shows a distributed cluster of correlation coefficients at around r = −0.567, −0.717, −0.477, −0.419, −0.210 and r = −0.488 respectively. We observed that high energy wavelet coefficient correlated well with bootstrap correlation, while low energy wavelet coefficient gives low bootstrap correlation. It was noticed that the geomagnetic storm has a influence on GIC and geomagnetic field derivatives (dB/dt). This might be ascribed to the coronal mass ejection with solar wind due to particle acceleration processes in the solar atmosphere.

1. Introduction

Solar disturbance (solar flare, coronal mass ejection and prominences) causes fluctuating currents in the ionosphere and magnetosphere. These currents produce geomagnetic variations and induce a geoelectric field which drives geomagnetically induced current (GIC) also known as telluric currents into the ground technological systems.

GIC are mostly noticed at the high latitude regions, the observed variations are related to the increase in the electrojets during the high ionospheric convection conditions and substorms current wedge enhancement during geomagnetic substorms. Kappenman (2003) observed that a huge sudden storm commencement (SSC) occurred on 24 March 1991 yielded the massive GIC observed in the United States. It was also noted that geomagnetic storm are affected by the enhancement of the ring current at low latitudes which developed large GICs (Kappenman, 2004). Viljanen et al. (1999), Boteler and Pirjola (1998) established that auroral electrojet, ionospheric current and magnetospheric current systems are

* Corresponding author.
E-mail addresses: olukayodefalayi@yahoo.com (E.O. Falayi), gbengadimu@googlemail.com (O. Ogunmodimu), oloriebimpjch2002@yahoo.co.uk (O.S. Bolaji), jacobayanda@yahoo.com (J.D. Ayanda), ojoniyi2013@gmail.com (O.S. Ojoniyi).

Peer review under responsibility of National Research Institute of Astronomy and Geophysics.

Production and hosting by Elsevier

http://dx.doi.org/10.1016/j.nrjag.2017.04.010
2090-9977/© 2017 Production and hosting by Elsevier B.V. on behalf of National Research Institute of Astronomy and Geophysics.

considered to be one of the principal causes of the geomagnetic disturbances leading to GIC. The basic challenges of GIC research are to identify, comprehend, and model the different geophysical processes similar with large GIC occurrence. Previous studies identified the various causes of GIC as storm sudden commencements (SSC), geomagnetic pulsations, and auroral substorms (Boteler, 2001; Lam et al., 2002; Pulkkinen et al., 2003, 2005).

Power system failures in different part of the world are affected by major geomagnetic disturbance (Boteler et al., 1998; Bolduc, 2002; Wik et al., 2009). Problems arise as results of the variations of the magnetic field induce currents in the power transmission lines. Literatures have shown the different geomagnetic storm values obtained in power networks located at different latitudes. Trivedi et al. (2007) presented Brazilian power network during geomagnetic disturbance between 7 and 8 November 2004 with GIC recordings to be 15 A and lasted for 5 h. Also, Watari et al. (2009) reported GIC value of 15 A between the year 2007 and 2009 in Japan. In China, Liu et al. (2009) reported GIC values of 47.2 A and 75.5 A related to the geomagnetic disturbance on 7–9 November 2004 respectively. The large geomagnetic disturbance was observed in 2003 which damage power transmission. The Swedish power system where the city of Malmo experienced a blackout for 20–50 min (Wik et al., 2008). In Scotland, Thomson et al. (2005) reported that 40 A of the GIC recorded during the disturbance on 30 October 2003. It was noticed that the geoelectric field was 50 times higher than quiet time during the geomagnetic disturbance event. In South Africa, 15 transformers were damaged by internal heating in November 2003, associated with the GIC production resulting from geomagnetic disturbances (Gaunt and Coetzee, 2007; Kappenman, 2005).

The Faraday's law described the drift of GIC, the significant quantity is the time derivative of the ground magnetic field (dB/dt), and proxy to the GIC values (Viljanen et al., 2001). Several studies have revealed the influence of GIC in high latitude regions, mostly affected by geomagnetic storm disturbances (Kappenman et al., 2000; Boteler, 2001; Erinmez et al., 2002; Pirjola, 2008; Pulkkinen et al., 2012; Viljanen et al., 2012; Falayi and Beloff, 2012; Falayi and Rabiu, 2013). Viljanen et al. (2001) examined dH/dt (exceeding 1 nT s^{-1}) using the IMAGE magnetometer data from North Europe between 1982 and 2001, it was observed that dH/dt is primarily significant during nighttime events governed by westward ionospheric currents. At mid latitude, Turnbull et al. (2009) studied 553 geomagnetic substorms between 2000 and 2003 during the year of solar maximum. They noticed the large dH/dt connected to westward ionospheric currents, but affected by smaller-scale ionospheric structures. Also, Viljanen and Tanskanen (2011) used dH/dt to examine the geomagnetic field variations at higher latitudes between 1983 and 2010. The dH/dt activity is high at both the midnight and early morning hours, disappear during the noon and afternoon phase.

In this paper, we analyze the geomagnetic storms that occurred on 31 March 2001, 21 October 2001, 6 November 2001, 29 October 2003, 31 October 2003 and 9 November 2004. Section 2 compared

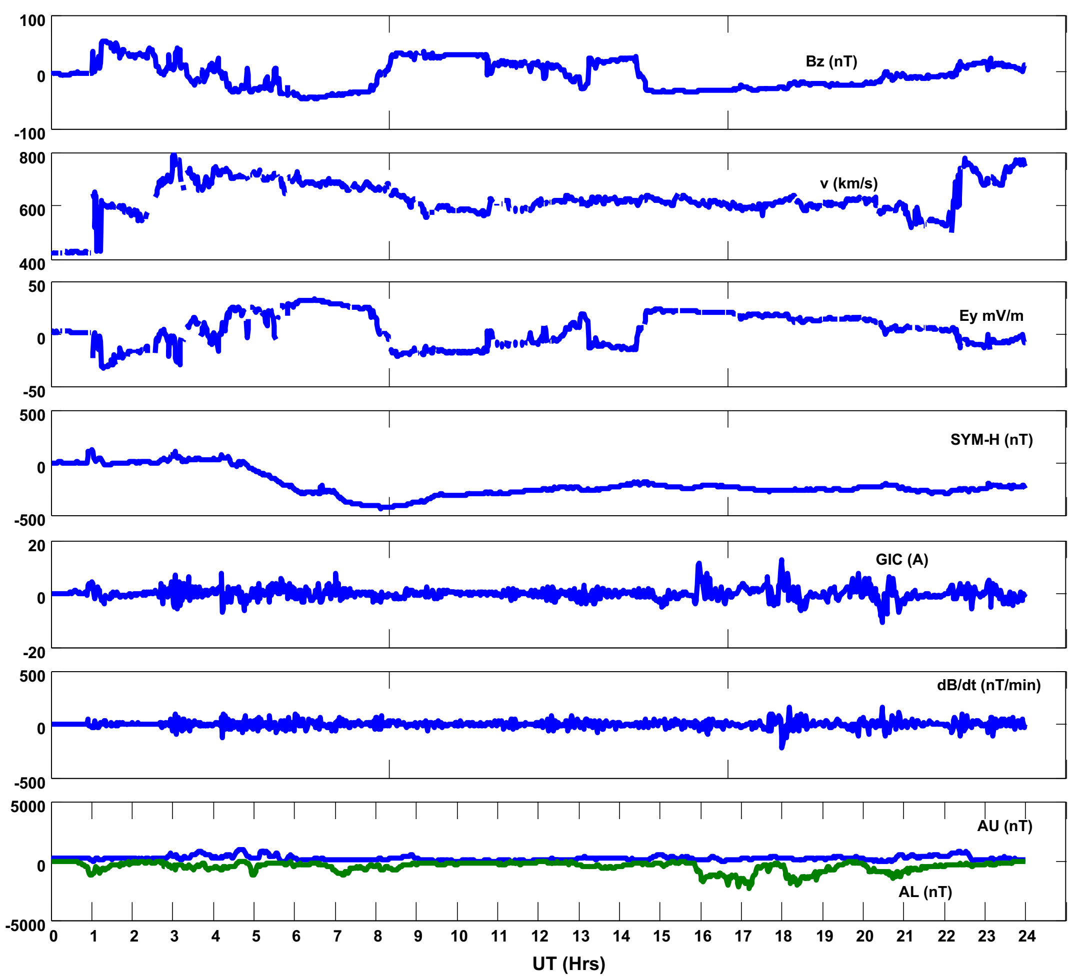

Fig. 1. Interplanetary parameters and geomagnetic parameters on 31 March 2001, Bz, v, Ey, SYM-H index, GIC, dB/dt, AU (blue line) and AL (green line) indices.

geomagnetic storm components of Bz (nT), v (km/s), Ey (mV/m), SYM-H (nT), GIC (A), dB/dt (nT/min), AU and AL (nT) indices. We examine the wavelet spectrum of geomagnetic induced current in Section 3. Section 4 provides a bootstrap method, regression correlations between the computed horizontal component of the time derivative of the geomagnetic field (dB/dt) and the measured values of the geomagnetically induced current (GIC). In Section 5 we discuss the results and Section 6 gives the conclusion.

2. Data sources and analysis methods

The data set used in present study are selected geomagnetic storms that occurred during the solar maximum events on 31 March 2001, 21 October 2001 and 6 November 2001, while on 29 October 2003, 31 October 2003 and 9 November 2004 are regarded as post solar maximum event, also based on the available GIC data during the geomagnetic storm events. The northward and eastward components of the geomagnetic field (X and Y) of the Nurmijarvi data, were collected from INTERMAGNET, http://www.intermagnet.org/. The GIC measurements were collected from Mantsala (60.381°N, 25.317°E), from where they were transferred to Nurmijarvi Geophysical Observatory (60.467°N, 24.8°E). Since the distance between Mantsala and Nurmijarvi is about 30 km, the natural variation fields are approximately identical on both sites. The following parameters used in these analyses were collected from OMNIWEB (http://omniweb.gsfc.nasa.gov) database includes; solar wind speed (v), gives the amplitude of the disturbance. The Bz (Interplanetary magnetic field, IMF), directed toward the south during the commencement of the geomagnetic storms. Symmetric disturbance field in H (SYM-H) index, AU (eastward electrojet) and AL (westward electrojet) indices using 1 min resolution data. Eq. (1) was used to obtain the geomagnetic field derivatives, which gives estimates of the induction (Viljanen et al., 2001).

$$\frac{dB}{dt} = \sqrt{\left(\frac{dB_X}{dt}\right)^2 + \left(\frac{dB_Y}{dt}\right)^2} \quad (1)$$

2.1. Magnetic storm of 31 March 2001

A magnetic storm was observed on 31 March 2001 with M 2.0 solar flare which occurred at 04:26 UT, maximum at 04:33 UT and ended at 04:37 UT. Fig. 1 shows the variation of the interplanetary magnetic field IMF (Bz), Solar wind speed (v), Electric field (Ey), Symmetric H (SYM-H), geomagnetically induced current (GIC), geomagnetic field derivatives (dB/dt), eastward and westward electrojet (AU and AL) indices. It was observed that the more negative values of SYM-H index, the more southward turning of Bz

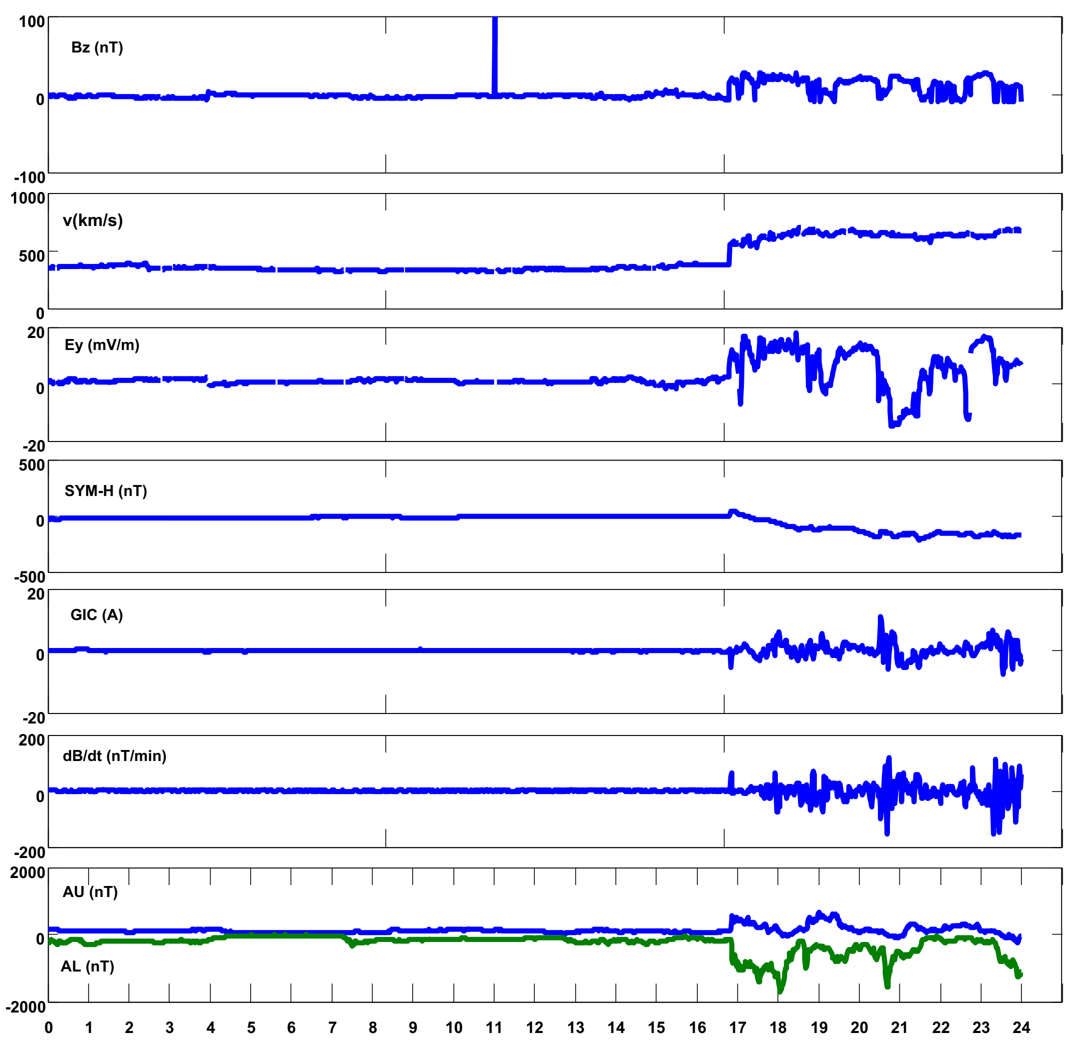

Fig. 2. Interplanetary parameters and geomagnetic parameters on 21 October 2001, Bz, v, Ey, SYM-H index, GIC, dB/dt, AU (blue line) and AL (green line) indices.

and reaches the minimum values of −47.77 nT at around 07:00 UT and maximum negative excursion of SYM-H index observed is −437 nT. Also, another change in polarity of Bz was noticed at 13:00 UT and 15:00 UT associated with another depression in SYM-H index with a solar wind speed of 790.2 km/s. As the Bz (pointed southward) value reaches its negative downward peak, the associated geomagnetic activity enhances. The variation of AU and AL was 978 nT and −2315 nT respectively. The effect of this substorms was clearly observed at the ground measurement of GIC and dB/dt with the values of 15.82 A and 162.477 nT/min respectively. The variation of the geoelectric field can lead to high values dB/dt and GIC.

2.2. Magnetic storm of 21 October 2001

Fig. 2 depicts the magnetic storm of 21 October 2001 with class M 2.5 solar flares at 11.25 UT and ends at 11:48 UT. A sudden storm commencement noted at 17:00 UT with an increase in solar wind velocities to about 705.7 km/s and IMF Bz showed strong southward variation with the minimum value of −11 nT. The electric field attained a peak value of 18.16 mV/m around 19:00 and 20:00 UT, another peak was noticed at 21:00 and 22:00 UT with the value 16 mV/m on the same day. The main phase of SYM-H index lasted for 8 h between 17:00 UT and 24:00 UT reaching a minimum value of −219 nT. The maximum values of GIC and dB/dt observed during the main phase are 11.29 A and 115.72 nT/min respectively.

2.3. Magnetic storm 6 November 2001

The data for Bz- of the interplanetary magnetic field, solar wind speed (v) and electric field (Ey) components were missing during the storm. Panels four to seven of Fig. 3 are symmetric disturbance index SYM-H, geomagnetic induced current GIC, time derivatives of geomagnetic field dB/dt and auroral indices (AU and AL) indices. The magnetic storm on 6 November 2001 with M1.2 solar flare event with active region of 9698, begin at 13:45:00 UT and maximum time was 13:51:00 UT and end at 14:05:00 UT was observed. We can notice that the minimum of Bz is −14 nT, while the amplitude of v and Ey are 736 km/s and 5.5 mV/m respectively. The main phase of SYM-H reaching a minimum value of −320 nT. The value of dB/dt and GIC are 203 nT/min and 31.6 A respectively at Nurmijarvi, Finland.

2.4. Magnetic storm 29 October 2003

The solar wind speed (v), interplanetary magnetic field (IMF) and electric field (Ey) measurements were unavailable during the Halloween events due to contamination. The magnetic storm on 29 October 2003 with X10 solar flare event with active region of 486, begin at 20:37:00 UT and maximum time was 20:49:00 UT and end at 21:01:00 UT was observed, and associated with halo coronal mass ejection. The main phase of SYM-H index lasted for 5 h between 8:00 UT and 13:00 UT reaching a minimum value of −364 nT. The value of dB/dt and GIC are 559 nT/min and 51.4 A respectively at Nurmijarvi, Finland (see Fig. 4).

2.5. Magnetic storm of 31 October 2003

The magnetic storm on 31 October 2003 with M2.0 solar flare event. The main phase of SYM-H index minimum value of −336 nT. The solar wind speed (v), interplanetary magnetic field

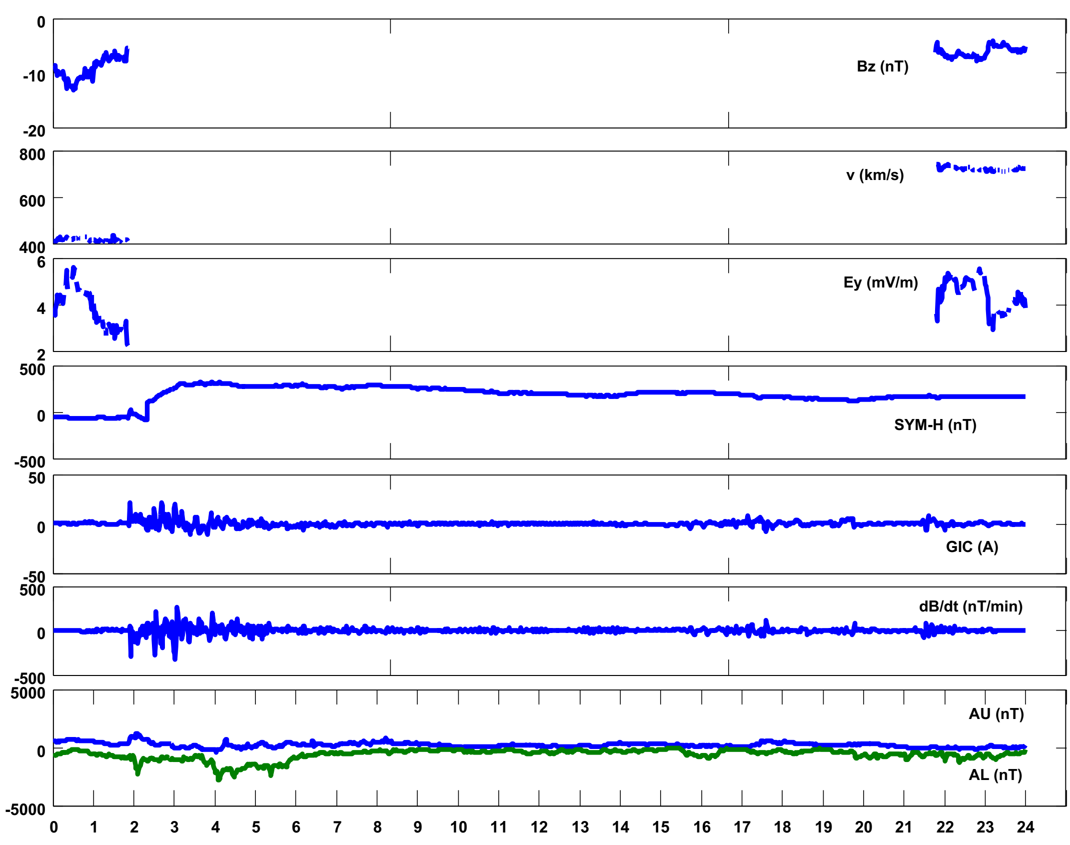

Fig. 3. Interplanetary parameters and geomagnetic parameters on 6 November 2001, Bz, v, Ey, SYM-H index, GIC, dB/dt, AU (blue line) and AL (green line) indices.

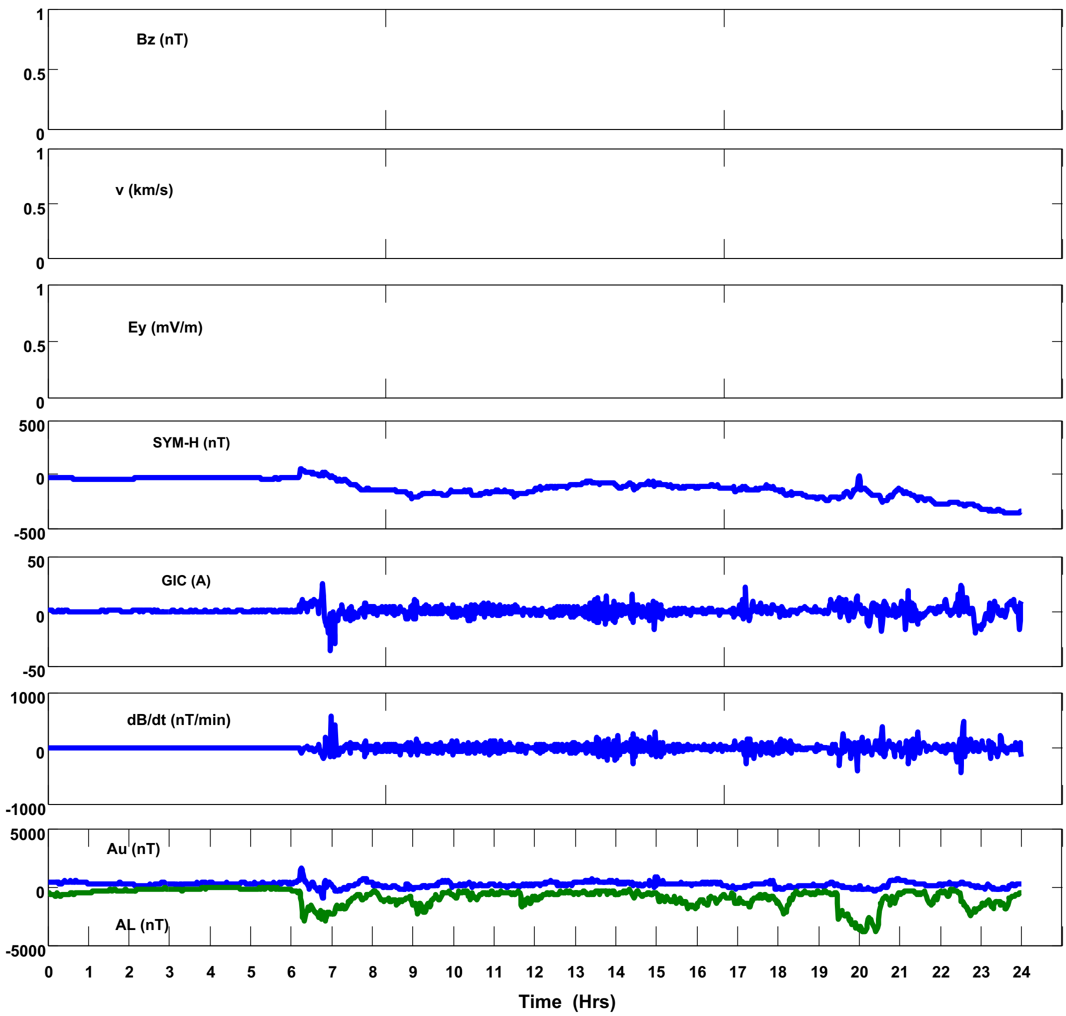

Fig. 4. Interplanetary parameters and geomagnetic parameters on 29 October 2003, Bz, v, Ey, SYM-H index, GIC, dB/dt, AU (blue line) and AL (green line) indices.

(IMF) and electric field (Ey) were missing at the beginning of the geomagnetic storm, However, we can observed that the Bz, v and Ey values are -4 nT, 1015 km/s and 4 mV/m respectively. The values of dB/dt and GIC are 287.8 nT/min and 30.1 A respectively (see Fig. 5).

2.6. Magnetic storm of 9 November 2004

Fig. 6 displays the response plot for 9 November 2004. The sudden storm commencement (SSC) is a signature for the appearance of a shock, which might have triggered the southward turning of Bz with deflection of the minimum peak value of -33.15 nT at 1900 UT. The solar wind speed increase from 600 km/s and shoot up to 845.4 km/s at 19:00 UT. The electric field (26.42 mV/m) coincides with solar wind and Bz. The electric fields (Ey) are important in the solar wind measurements for the production of geomagnetic disturbance. The arrivals of a shock in the interplanetary medium have an influence on the depression of the SYM-H index with a minimum peak value of -271 nT. The AU and AL values showed large fluctuations when Bz values turned negative with an increase in solar wind speed with a large depression in SYM-H. The value of dB/dt and GIC are 416.64 nT/min and 42.82 A respectively at Nurmijarvi, Finland. Compared to the intensity of the March 13, 1989, in which disturbance triggered the Hydro-Quebec collapse with a value of 479 nT/min for 9 h (Kappenman, 2006).

3. Wavelet spectrum analysis of GIC

Small packets of waves are referred to as wavelet, wavelets can be stretched and translated in both frequency and time, with a flexible resolution and they can easily map changes in the time frequency area. Nowadays, several researchers are using a wavelet spectrum analysis approach to examine space weather data. Wavelet analysis is a strong instrument to investigate the dominant mode of variation and to evaluate how it changes with time, by breaking down a nonlinear time series into time frequency space. Morlet wavelet is a wavelet composed of a compound exponential function of frequency whose amplitude is modulated by a function proportional to the standard Gaussian. The Morlet wavelets are produced in term of translation and dilation of fixed function. The dilation of the Morlet function generates low duration, high frequency, high duration and low frequency functions. The functions can be used to represent low bursts of long frequency or long duration slowly varying signals.

Several literatures revealed the appropriate technical details used in mother wavelets transformation (Torrence and Compo, 1998). The wavelet transform of a function Ψ (a, x) (t) derived from the mother wavelet Ψ (t) by dilation and translation.

$$\psi_{a,b} = \frac{1}{a^{1/2}}\psi\left(\frac{t-x}{a}\right) \quad (2)$$

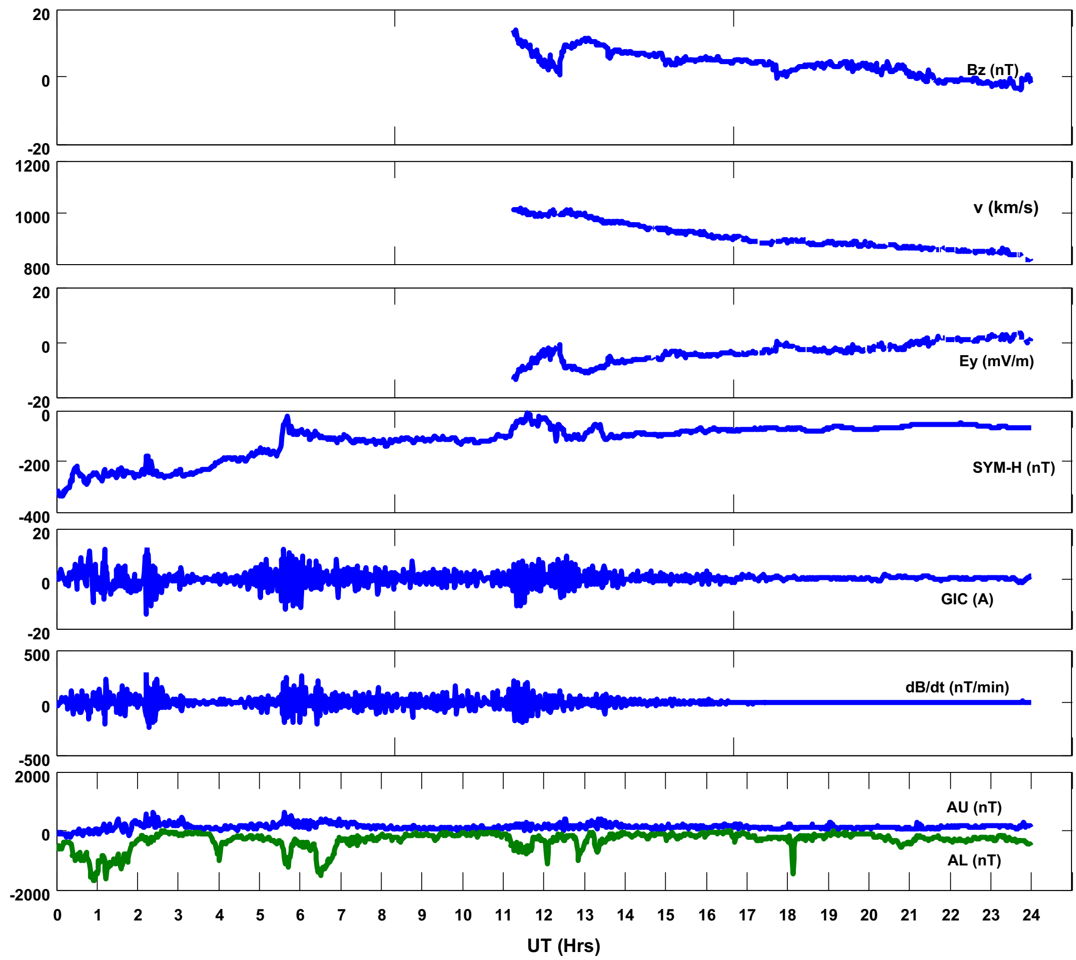

Fig. 5. Interplanetary parameters and geomagnetic parameters on 31 October 2003, Bz, v, Ey, SYM-H index, GIC, dB/dt, AU (blue line) and AL (green line) indices.

where x is the position that is translated and considered to be scale dilation. The wavelet transformation of the mother wavelet Ψ (t) is the convolution integral is

$$W(b,a) = \frac{1}{a^{1/2}} \int \psi^* \left(\frac{t-x}{a}\right) \psi(t) dt \quad (3)$$

where ψ∗ is the conjugate of ψ. While the morlet wavelet is known to be mother wavelet Ψo given by

$$\psi_o(t) = \pi^{-1/4} \exp(iwt) \exp(-t^2/2) \quad (4)$$

where t is the time and ω is the wave number (Torrence and Compo, 1998). The work presented in this section uses the wavelet spectrum to analyze the geomagnetic induced current on 31 March 2001, 21 October, 2001, 6 November 2001, 29 October 2003, 31 October 2003 and 9 November 2004 (Fig. 7a–f).

4. Estimates of the regression coefficients

Bootstrapping is a statistical method used to assess the accuracy of the model such as the standard error, confidence interval and the bias of an estimator. The bootstraps utilize the values of the independent and dependent variables as the population and the estimates of the sample as accurate values. The important inference of bootstrapping is that the sample distribution is a strong estimation to the population distribution. It can be used for statistics with sampling distributions that are complex to obtain (Efron and Tibshirani, 1993). In this section, we use the bootstrap method to obtain a better estimate of regression coefficients between the geomagnetic field derivatives from Eq. (1) and observed values of the geomagnetically induced current (GIC) on the geomagnetic storm events. When the subsamples outlier gives strong correlation (close to 1) this implies strong relationship between the parameters, while subsamples without the outlier produce low values of correlation coefficient, recommending no interrelationship between the parameters (Trauth, 2010).

5. Discussion

The Bz IMF components have greater impact on auroral electrojets, this is also demonstrated in the geomagnetic disturbance strength. The greatest influence on auroral electrojets is due to changes of the Bz IMF component during geomagnetic storm strength. During the burst of sudden storm commencement, it was also observed that the solar wind is significant with the southward Bz IMF at the period of the main phase of the magnetic storm. The ionospheric dynamo is considered as part of the important parameters in the generation of ionospheric current and electric fields. When the dynamo is disturbed during the storm, it produces an ionospheric electric current and electric field at the high latitude. The ionospheric current subsequently produces variation in the geomagnetic field and has impact on geomagnetically induced currents (see Figs. 1–6). It was observed that the GIC and the

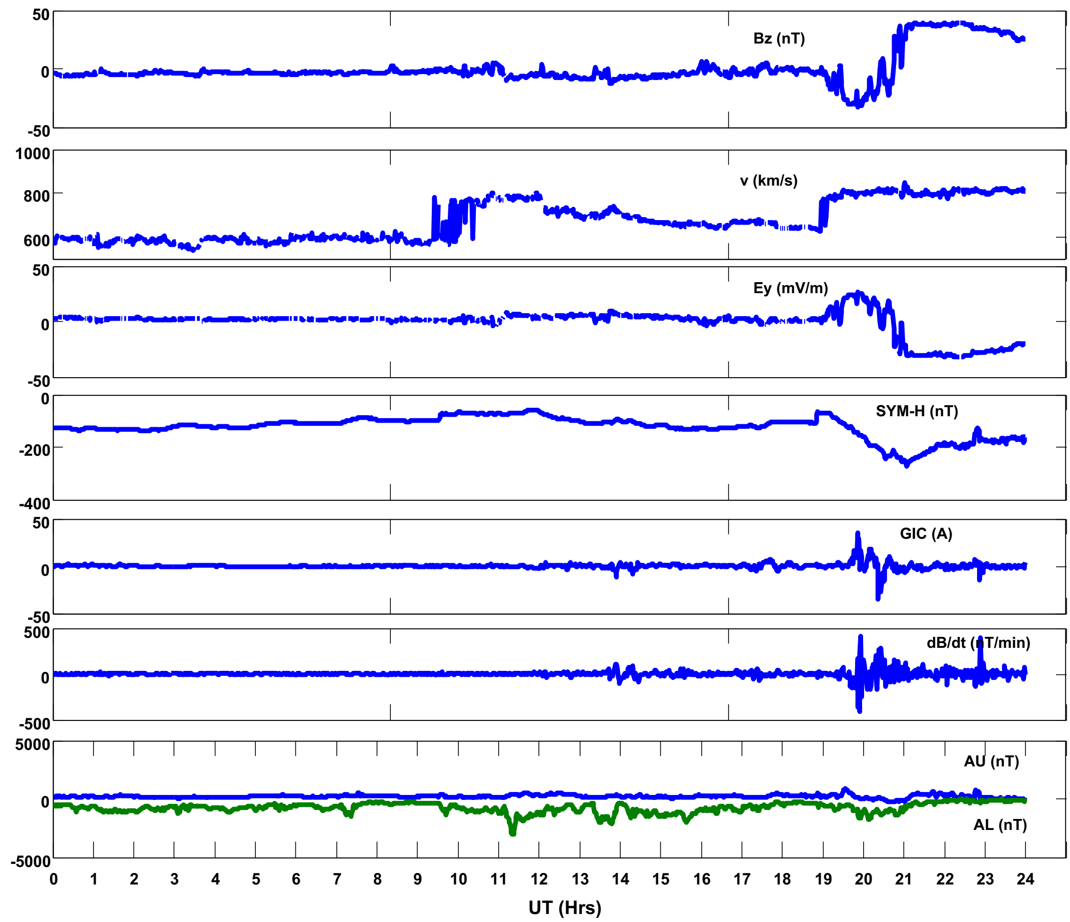

Fig. 6. Interplanetary parameters and geomagnetic parameters on 9 November 2004, Bz, v, Ey, SYM-H index, GIC, dB/dt, AU (blue line) and AL (green line) indices.

derivatives of geomagnetic field on 31 March 2001, 21 October 2001 and 9 November 2004 show the same signature with solar wind and geomagnetic index parameters. Morning-time enhancement of the geomagnetic storms were observed on 6 November 2001, 29 October 2003, 31 October 2003 of the geomagnetic storm. The geomagnetic storm on 21 October 2001 and 9 November 2004 events were dominant at night-time. The loading and unloading of energy leading to the substorms electrojet have an influence on the geomagnetic field variation. The major driver of the GIC in the higher latitudes is the ionospheric electric current system is linked to the high scale magnetospheric and solar wind dynamics (Akasofu and Merrit, 1979). These variations are thought to be related to the intensification of the electrojets during enhanced ionospheric convection conditions.

We applied the wavelet-based method to analyze the GIC time series on 31 March 2001, 21 October 2001, 6 November 2001, 29 October 2003, 31 October 2003 and 9 November 2004, observed in a sequence of time scales of one to twenty four hours, using the sampling intervals described above. Fig. 7(a–f) depicts the wavelet power spectra for the daily GIC at Nurmijarvi geophysical observatory. It was observed that there are more concentration of power between the 14–24 h on 31 March 2001, 17–24 h on 21 October 2001, 1–7 h on 6 November 2001, two peaks were observed between 5–8 h and 21–24 h on 29 October 2003, 1–3 h on 31 October 2003 and 18–22 h on 9 November 2004, which shows that this time series have a strong signal, with a confidence level of 95% (Torrence and Compo, 1998). The significant peaks in the GIC power spectra are shown in Fig. 7 for the wavelet analysis. It was observed that all fluctuations have a signature of the scaling spectral exponent computed by linear regression fitting of the scaling GIC date. We noted that disturbance periods are featured by high wavelet coefficients of geomagnetic storms on 31 March, 2001, 21 October 2001, 6 November 2001, 29 October 2003 and 9 November 2004 (see Fig. 7a–d and f). Low wavelet coefficients of geomagnetic storms were observed on 31 October 2003 (Fig. 7e). The higher energy wavelet coefficients are more significant at a high frequency this is might be influenced by the strong ionospheric currents at Nurmijarvi. This wavelet spectrum provides impartial and stable estimation of the power spectrum and it is a better way to characterize the time series variability. The enhancement of the GIC might depend on temporal and spatial structure of the magnetospheric and ionospheric electric currents source and distribution of the conductivity in the Earth (see Fig. 7a–d and f) (Boteler, 2001; Kappenman, 2003; Pulkkinen et al., 2005). Also, GIC are influenced by current systems that vary rapidly with time and also assumed to be related with the main phase of the geomagnetic storm.

Fig. 8(a–c) depict the sample distribution of correlation coefficients for each day of the storm events. The bootstrap samples were obtained from the random sample, we consider the interrelationship based on the sample between the GIC and dB/dt on 31 March 2001, 21 October 2001, 6 November, 29 October 2003, 31 October 2003 and 9 November 2004, which shows an approximately distributed cluster of correlation coefficients at around r = −0.567, −0.717, −0.477, −0.419, −0.210 and r = −0.488 respectively. We obtain negative correlations between observed geomag-

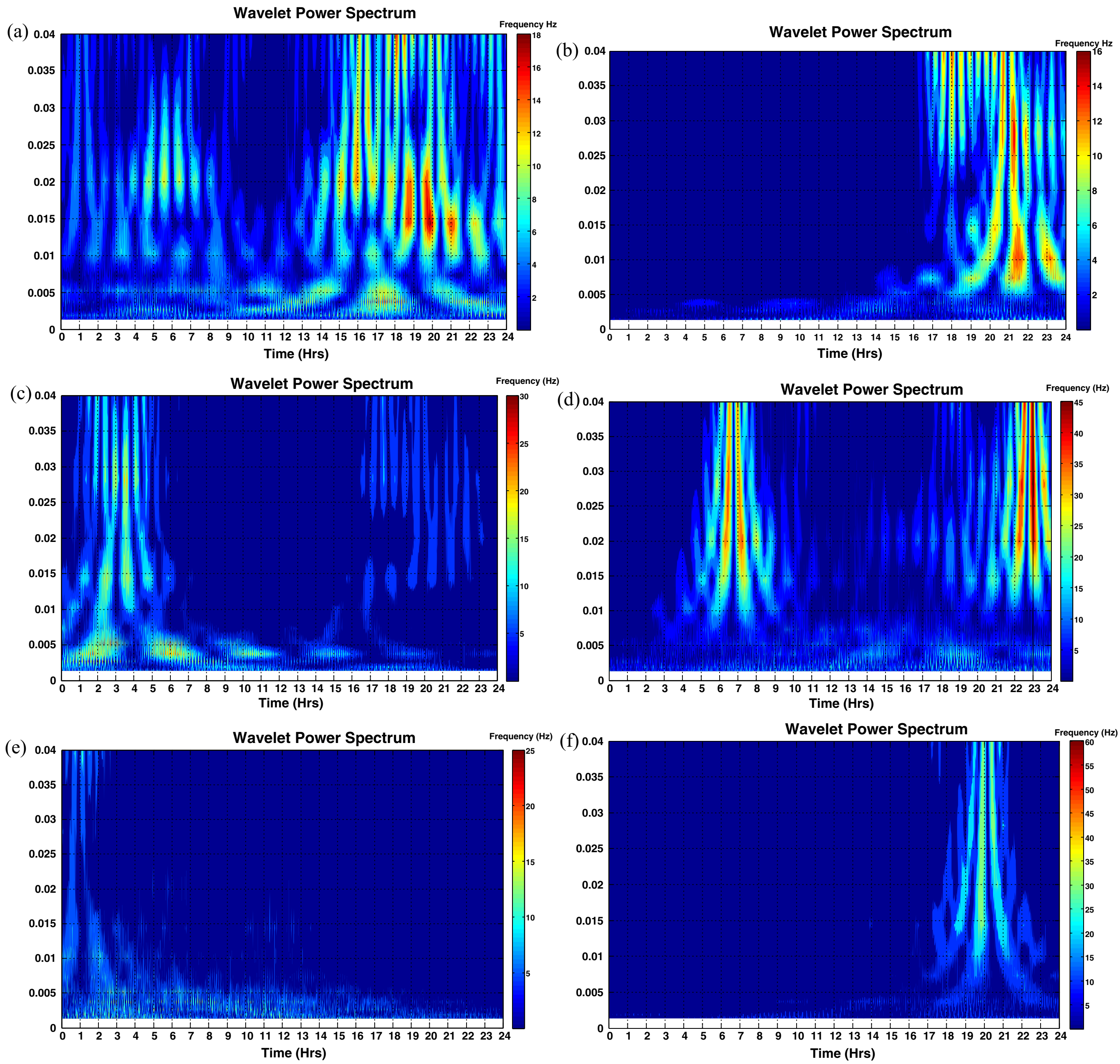

Fig. 7. (a–f). Wavelet spectrum analyses of the geomagnetic induced current on (a) 31 March 2001 (b) 21st October 2001 (c) 6 November 2001 (d) 29 October 2003 (e) 31 October 2003 and (f) 9 November 2004.

netic induced current and time derivatives of the geomagnetic field (dB/dt). It was noticed that the geomagnetic storm has a influence on GIC and geomagnetic field derivatives (dB/dt). This might be ascribed to the coronal mass ejection with solar wind due to particle acceleration processes in the solar atmosphere. We observed that high energy wavelet coefficient correlated well with bootstrap correlation, while low energy wavelet coefficient gives low bootstrap correlation.

6. Conclusions

This study is to describe both the geomagnetic induced current (GIC) and time derivatives of the geomagnetic field (dB/dt) events that occurred in Finland on the three geomagnetic storm on 31 March 2001, 21 October 2001, 6 November 2001, 29 October 2003, 31 October 2003 and 9 November 2004. There is more concentration of power between the 14–23 h on 31 March 2001, 17–24 h on 21 October 2001, 1–7 h on 6 November 2001, two peaks were observed between 5–8 h and 21–24 h on 29 October 2003, 1–3 h on 31 October 2003 and 18–22 h on 9 November 2004, using the wavelet spectral approach for the GIC. It was shown that the time series has a strong signal within a confidence level of 95% (Torrence and Compo, 1998). Bootstrap method regression exhibits negative correlations between the time derivative of the geomagnetic field (dB/dt) and the observed values of the geomagnetic induced current. We noticed that high energy wavelet coefficient correlated well with bootstrap correlation, while low energy wavelet coefficient gives low bootstrap correlation.

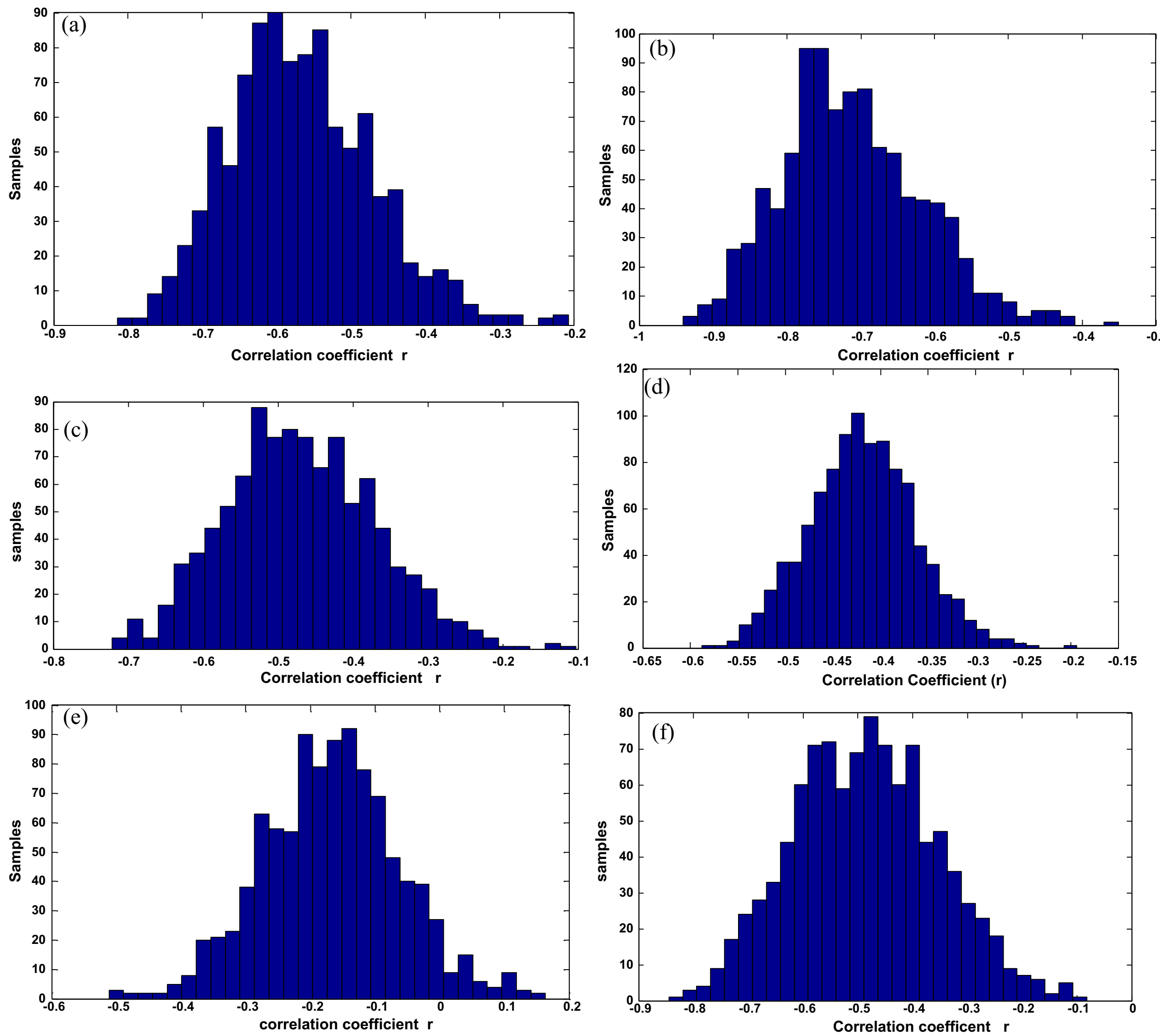

Fig. 8. (a–f): Bootstrap method regression correlations between the computed horizontal component of the time derivative of the geomagnetic field (dB/dt) and the observed values of the geomagnetic induced current (GIC) on (a) 31 March 2001 (b) 21 October 2001 (c) 6 November 2001 (d) 29 October 2003 (e) 31 October 2003 and (f) 9 November 2004.

Acknowledgement

The authors acknowledge the OMINIWEB (http://www.omniweb.gsfc.nasa.gov) staff for providing v, Bz, SYM-H, AU, and AL. We appreciate INTERMAGNET for providing geomagnetic field data (http://www.intermagnet.org/data). We would also like to thank Finnish Meteorological Institute, Space Research Unit, Helsinki, Finland, for the provision of the geomagnetically induced current data.

References

Akasofu, S.I., Merritt, R.P., 1979. Electric Currents in Power Transmission Lines Induced by Auroral Activity. Nature 279, 308.

Boteler, D.H., Pirjola, R.J., 1998. The complex-image method for calculating the magnetic and electric fields produced at the surface of the Earth by the auroral electrojet. Geophys. J. Int. 132, 31–40.

Boteler, D.H., Pirjola, R.J., Nevanlinna, H., 1998. Th. effects of geomagnetic disturbances on electrical systems at the Earth's surface. Adv. Space Res. 22, 17–27.

Boteler, D., 2001. Assessment of geomagnetic hazard to power systems in Canada. Nat. Hazard. 23, 101–120. http://dx.doi.org/10.1023/A:1011194414259.

Bolduc, L., 2002. GIC observations and studies in the Hydro-Quebec power system. J. Atmos. Sol. Terr. Phys. 64 (16), 1793–1802.

Erinmez, I.A., Kappenman, J.G., Radasky, W.A., 2002. Management of the geomagnetically induced current risks on the national grid company's electric power transmission system. J. Atmos. Terr. Phys. 64, 743–756.

Efron, B., Tibshirani, R.J., 1993. An Introduction to the Bootstrap. Chapman and Hall, New York.

Falayi, E.O., Beloff, N., 2012. Modelling of geomagnetically induced currents during geomagnetic storms using geoelectric fields and auroral electrojet indices. Indian J. Phys. 86 (6), 423–429. http://dx.doi.org/10.1007/s12648-012-0108-0.

Falayi, E.O., Rabiu, A.B., 2013. Dependence of time derivative of horizontal geomagnetic field on sunspot number and aa index. Acta Geophys. 61, 211–222.

Gaunt, C.T., Coetzee, G., 2007. Transformer failures in regions incorrectly considered to have low GIC-risk. In: IEEE Power Tech Conference Paper 445.

Kappenman, J., Radasky, W., Gilbert, J., Erinmez, L., 2000. Advanced geomagnetic storm forecasting: a risk management tool for electric power system operations. IEEE Trans. Plasma Sci. 28 (6), 2114–2121. http://dx.doi.org/10.1109/27.902238.

Kappenman, J.G., 2004. The evolving vulnerability of electric power grids. SpaceWeather 2, S01004. http://dx.doi.org/10.1029/2003SW000028.

Kappenman, J.G., 2003. Storm sudden commencement events and the associated geomagnetically induced current risks to ground based systems at low-latitude and midlatitude locations. Space Weather 1, 1000–1016. http://dx.doi.org/10.1029/2003SW000009.

Kappenman, J.G., 2005. An overview of the impulsive geomagnetic field disturbances and power grid impacts associated with the violent sun-earth connection events of 29–31 October 2003 and a comparative evaluation with

other contemporary storms. Space Weather 3. S08C01. 10.1029/2004SW000128.
Kappenman, J.G., 2006. Great geomagnetic storms and extreme impulsive geomagnetic field disturbance events, an analysis of observational evidence including the great storm of May 1921. Adv. Space Res. 38, 188–199. http://dx.doi.org/10.1016/j.asr.2005.08.055.
Lam, H.L., Boteler, D.H., Trichtchenko, L., 2002. Case studies of space weather events from their launching on the Sun to their impacts on power systems on the Earth. Ann. Geophys. 20, 1073–1079.
Liu, C.M., Liu, L.G., Pirjola, R., 2009. Geomagnetically induced currents in the high-voltage power grid in China. IEEE Trans. Power Delivery 24, 1–4.
Pirjola, R., 2008. Effects of interactions between stations on the calculation of geomagnetically induced currents in an electric power transmission system. Earth Planets Space 60, 743–751.
Pulkkinen, A., Amm, O., Viljanen, A.BEAR Working Group, 2003. Ionospheric equivalent current distributions determined with the method of spherical elementary current systems. J. Geophys. Res. 108 (A2), 1053. http://dx.doi.org/10.1029/2001JA005085.
Pulkkinen, A., Lindahl, S., Viljanen, A., Pirjola, R., 2005. Geomagnetic storm of 29–31 October 2003: Geomagnetically induced currents and their relation to problems in the Swedish high voltage power transmission system. Space Weather 3, S08C03. http://dx.doi.org/10.1029/2004SW000123.
Pulkkinen, A., Bernabeu, E., Eichner, J., Beggan, C., Thomson, A.W.P., 2012. Generation of 100-year geomagnetically induced current scenarios. Space Weather 10, S04003. http://dx.doi.org/10.1029/2011SW000750.
Thomson, A.W.P., McKay, A.J., Clarke, E., Reay, S.J., 2005. Surface electric fields and geomagnetically induced currents in the Scottish Power grid during the 30 October 2003 geomagnetic storm. Space Weather 3, S11002. http://dx.doi.org/10.1029/2005SW000156.
Trivedi, N.B., Vitorello, Í., Kabata, W., Dutra, S.L.G., Padilha, A.L., Bologna, M.S., de Pádua, M.B., Soares, A.P., Luz, G.S., de A Pinto, F., Pirjola, R., Viljanen, A., 2007. Geomagnetically induced currents in an electric power transmission system at low latitudes in Brazil: a case study. Space Weather 5 (4), S04004. http://dx.doi.org/10.1029/2006SW000282.
Torrence, C., Compo, G.P., 1998. A practical guide to wavelet analysis. Bull. Am. Met. Soc. 79 (1), 61–78.
Turnbull, K.L., Wild, J.A., Honary, F., Thomson, A.W.P., McKay, A.J., 2009. Characteristics of variations in the ground magnetic field during substorms at mid latitudes. Ann. Geophys. 27, 3421–3428.
Trauth, M.H., 2010. Matlab Recipes for Earth Science. Springer-Verlag, Berlin, Germany, pp. 50–155.
Viljanen, A., Amm, O., Pirjola, R., 1999. Modelling geomagnetically induced currents during different ionospheric situations. J. Geophys. Res. 104 (28059–28), 072.
Wik, M., Viljanen, A., Pirjola, R., Pulkkinen, A., Wintoft, P., Lundstedt, H., 2008. Calculation of geomagnetically induced currents in the 400 kV power grid in southern Sweden. Space Weather 6, S07005. http://dx.doi.org/10.1029/2007SW000343.
Wik, M., Pirjola, R., Lundstedt, H., Viljanen, A., Wintoft, P., Pulkkinen, A., 2009. Space weather events in July 1982 and October 2003 and the effects of geomagnetically induced currents on Swedish technical systems. Ann. Geophys. 27, 1775–1787.
Watari, S., Kunitake, M., Kitamura, K., Hori, T., Kikuchi, T., Shiokawa, K., Nishitani, N., Kataoka, R., Kamide, Y., Aso, T., Watanabe, Y., Tsuneta, Y., 2009. Measurements of geomagnetically induced current in a power grid in Hokkaido, Japan. Space Weather 7, S03002. http://dx.doi.org/10.1029/2008SW000417.
Viljanen, A., Tanskanen, E., 2011. Climatology of rapid geomagnetic variations at high latitudes over two solar cycles. Ann. Geophys. 29, 1783–1792.
Viljanen, A., Nevanlinna, H., Pajunpaa, K., Pulkkinen, A., 2001. Time derivative of the horizontal geomagnetic field as an activity indicator. Ann. Geophys. 19, 1107–1118.
Viljanen, A., Pirjola, R., Wik, M., Ádám, A., Prácser, E., Sakharov, Y., Katkalov, J., 2012. Continental scale modelling of geomagnetically induced currents. J. Space Weather Space Clim. 2, A17. http://dx.doi.org/10.1051/swsc/2012017.